© 2016. Published by The Company of Biologists Ltd | Journal of Experimental Biology (2016) 219, 1458-1466 doi:10.1242/jeb.134924

RESEARCH ARTICLE

Sperm chemotaxis promotes individual fertilization success in sea urchins

Yasmeen H. Hussain[1], Jeffrey S. Guasto[2], Richard K. Zimmer[3], Roman Stocker[4] and Jeffrey A. Riffell[1,*]

ABSTRACT

Reproductive success fundamentally shapes an organism's ecology and evolution, and gamete traits mediate fertilization, which is a critical juncture in reproduction. Individual male fertilization success is dependent on the ability of sperm from one male to outcompete the sperm of other males when searching for a conspecific egg. Sperm chemotaxis, the ability of sperm to navigate towards eggs using chemical signals, has been studied for over a century, but such studies have long assumed that this phenomenon improves individual male fitness without explicit evidence to support this claim. Here, we assessed fertilization changes in the presence of a chemoattractant-digesting peptidase and used a microfluidic device coupled with a fertilization assay to determine the effect of sperm chemotaxis on individual male fertilization success in the sea urchin *Lytechinus pictus*. We show that removing chemoattractant from the gametic environment decreases fertilization success. We further found that individual male differences in chemotaxis to a well-defined gradient of attractant correlate with individual male differences in fertilization success. These results demonstrate that sperm chemotaxis is an important contributor to individual reproductive success.

KEY WORDS: Fertilization ecology, Gamete interactions, Microfluidics, Sperm competition

INTRODUCTION

Sperm competition is a significant force in the evolution of male reproductive traits and critically important in individual male reproductive success (Engqvist, 2013; Birkhead and Moller, 1998). In particular, gamete characteristics operating at the scale of a single cell have been shown to mediate population- and individual-level differences in reproduction (Simmons and Fitzpatrick, 2012; Snook, 2005; Fitzpatrick et al., 2012; Fitzpatrick and Lüpold, 2014; Simpson et al., 2014; Levitan, 2000; van der Horst and Maree, 2014). Sea urchin males with faster sperm have greater fertilization success (Levitan, 2000) and, in low sperm concentration situations, marine tube worm sperm head length correlates with relative fitness (Johnson et al., 2013). Gamete recognition factors are also known to play a role in sperm competition and fertilization success (Swanson and Vacquier, 2002; Palumbi, 1999; Zigler et al., 2005). For example, within the same species, sea urchin eggs are far more likely to be fertilized by sperm with closely related alleles for the recognition protein bindin than by sperm with divergent bindin alleles (Palumbi, 1999), and gamete compatibility between different sea urchin species can be explained by bindin relatedness (Zigler et al., 2005). The interplay between sperm traits, behavior and chemosensory processes is fundamental in regulating gamete interactions and fertilization. While sperm motility, morphology and biochemical factors have been shown to influence fertilization success, a direct link between the chemotactic navigation abilities of sperm and fertilization success remains elusive.

Chemical communication is suspected to be one of the many prezygotic forces operating to affect successful fertilization (Riffell et al., 2004; Evans and Sherman, 2013). Increasing evidence from a wide variety of taxa, ranging from marine invertebrate broadcast spawners to terrestrial internal fertilizers and plants, suggests that sperm chemotaxis to conspecific eggs is a common phenomenon (Brokaw, 1957; Spehr et al., 2003; Eisenbach, 1999; Yoshida et al., 2008). Recent studies have suggested that egg-derived chemoattractants specifically increase interaction and fertilization with compatible sperm (Riffell et al., 2004; Fitzpatrick et al., 2012; Oliver and Evans, 2014). For instance, abalone sperm chemotactically respond only to conspecific eggs, and the presence of chemoattractant gradients originating from abalone eggs increases fertilization success (Riffell et al., 2004). Individual male mussels have sperm that preferentially orient towards the particular females with which they are most genetically compatible (Evans et al., 2012). Preferential chemoattraction of sperm to conspecific eggs suggests that sperm chemoattractant responses may have a role in the evolution of gamete traits in broadcast spawners (Oliver and Evans, 2014; Evans and Sherman, 2013), but the effect of sperm chemoattraction on individual fertilization success has remained unknown.

Broadcast-spawning marine invertebrates, particularly sea urchins, are excellent models for testing the correlation between sperm chemotactic behavior and individual male fertilization success. The sea urchin *Arbacia punctulata* has been used in studies of fertilization and embryo development since the late 1800s, because of the large numbers of gametes each animal produces and their ease of manipulation in a laboratory (Harvey, 1956). The first published experiments on animal sperm accumulation to conspecific eggs were conducted in *A. punctulata* in 1912 (Lillie, 1912). The attractants for the species *Strongylocentrotus purpuratus* (Watkins et al., 1978), *Lytechinus pictus* (Kopf et al., 1979; Hansbrough and Garbers, 1981) and *A. punctulata* (Suzuki et al., 1984; Ward et al., 1985) were identified decades later, and the physiology and molecular mechanisms of sea urchin sperm chemotaxis have been well studied since then (Kaupp et al., 2006; Darszon et al., 2008; Yoshida and Yoshida, 2011). Other factors affecting fertilization success in sea urchins have also been explored: gamete recognition proteins have been identified and their effects on fertilization characterized in *A. punctulata* (Schmell et al., 1977), *S. purpuratus* (Vacquier and Moy, 1977) and related species (Metz et al., 1998; Lessios et al., 2012; Zigler et al., 2005; Levitan, 2012;

[1]University of Washington, Department of Biology, Seattle, WA 98195, USA. [2]Tufts University, Department of Mechanical Engineering, Medford, MA 02155, USA. [3]University of California Los Angeles, Department of Ecology and Evolutionary Biology, Los Angeles, CA 90095, USA. [4]ETH Zurich, Department of Civil, Environmental and Geomatic Engineering, Zurich 8093, Switzerland.

*Author for correspondence (jriffell@uw.edu)

Received 5 December 2015; Accepted 24 February 2016

Journal of Experimental Biology (2016) 219, 1458-1466 doi:10.1242/jeb.134924

Palumbi, 1999). The large body of research on fertilization and chemoattraction in sea urchins makes this an excellent model system to study the effects of chemoattraction on individual fertilization success.

Identifying the links between sperm chemoattraction and male fitness requires fine-scale control of the attractant conditions in parallel with the ability to identify differential male reproductive success. In this study, we used microfluidic devices and video microscopy of sperm chemotactic behavior to well-defined, spatiotemporal attractant gradients in combination with experimental manipulations of chemoattractant gradients around live eggs in fertilization bioassays. The results of our experiments demonstrate that individual fertilization success is an important contributor to sperm chemotactic ability.

MATERIALS AND METHODS

We investigated the effect of sperm chemoattraction on male fertilization success using two approaches: first by removing sperm chemoattractant from eggs and measuring the resulting difference in fertilization (Fig. 1A), then by comparing sperm navigation towards the chemoattractant gradient generated in a microfluidic device to individual male fertilization success (Fig. 1B,C).

Sea urchin gamete collection

Lytechinus pictus (Verrill 1867) sea urchins were purchased during their gravid season of May–October (South Coast Bio-Marine, San Pedro, CA, USA) and held in a dedicated seawater room (8–10°C, 75 l tanks) for up to 2 months, during which time they were supplied with kelp (*Nereocystis luetkeana*) and sea lettuce (*Ulva* spp.) collected from Shilshole Bay, WA, USA. Both male and female gametes were collected using standard protocols: 0.5–1.0 ml of 0.5 mol l^{-1} KCl was injected into the coelomic cavity (Strathmann, 1987; Harvey, 1956). Sperm were collected dry and stored on ice for use within 8 h. Eggs were spawned by female inversion onto a beaker containing 35 ml artificial seawater (ASW) made as described by Guerrero et al. (2010). Eggs from 2–4 females were

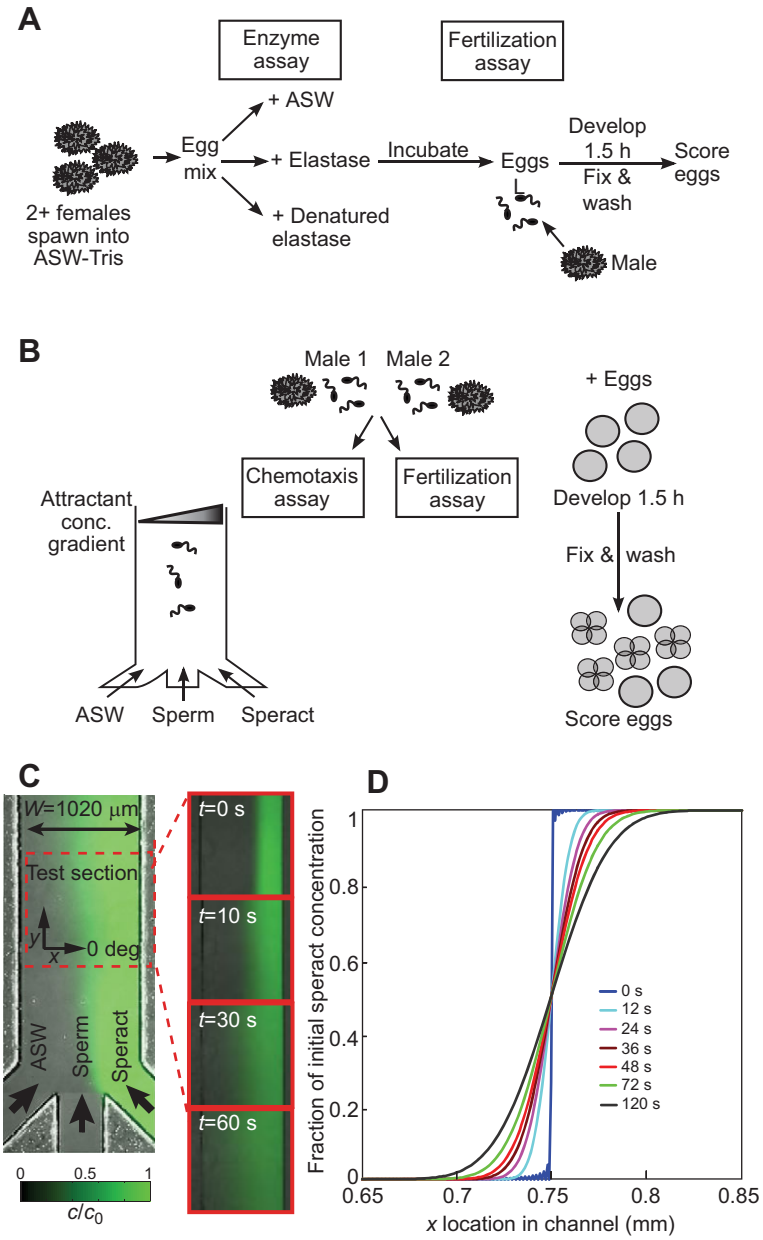

Fig. 1. Experimental methods and microfluidic device used in chemotaxis assays. (A) The effect of chemoattraction on fertilization was determined by digesting attractant with elastase and comparing fertilization success. The performance of elastase-exposed eggs was compared with that of eggs incubated in denatured elastase, as well as artificial seawater (ASW). (B) The relationship between chemotaxis and fertilization success was determined by comparing sperm performance in a microfluidic-based chemotaxis assay (depicted in C) with the percentage of eggs fertilized by the corresponding males. (C) Microfluidic channel used in the chemotaxis assay. Left, the microfluidic channel was 1020 µm wide and 99 µm deep. Video images of sperm in the channel were recorded 5 mm from the inlet. Right, the microfluidic channel allowed precise experimental and computational determination of the speract concentration (c/c_0) in the channel. (D) The starting speract concentration used for the chemotaxis assay was c_0=1.39×10^{-9} mol l^{-1}, and speract diffusion in the channel was determined by the advection–diffusion equation and confirmed experimentally with measurements of diffusion of 10^{-4} mol l^{-1} fluorescein used in place of attractant (C, left). To account for the difference in diffusion coefficients between fluorescein (D=5×10^{-10} m^2 s^{-1}) and speract (D=3×10^{-10} m^2 s^{-1}), time was scaled by the ratio of the diffusion coefficients.

Journal of Experimental Biology (2016) 219, 1458-1466 doi:10.1242/jeb.134924

pooled together in equal ratios to minimize individual female variability.

Fertilization assays

In all experiments, we examined the fertilization success between individual males as the initial step towards determining the correlation between sperm chemotaxis and fertilization. Prior to fertilization experiments, gamete concentrations were quantified in a hemocytometer, and the measured concentrations were used to control sperm:egg ratios in the fertilization bioassays (Lillie, 1915; Riffell et al., 2004; Schmell, 1977). Sperm:egg ratios of 100:1, 300:1 and 1000:1 (number of eggs=1513±356; number of sperm=$2\times10^5\pm3.3\times10^4$ at 100:1, $7.2\times10^5\pm1.6\times10^5$ at 300:1, $1.8\times10^6\pm2.3\times10^5$ at 1000:1) were added to the wells of a 24-well plate (Falcon Clear Polystyrene Sterile Tissue Culture Multiwell Plate, BD Biosciences, San Jose, CA, USA), yielding 8 replicates for each treatment and male at each sperm:egg ratio. To control for contact time, 1 ml of 0.5 mol l^{-1} KCl solution was added to stop sperm motility (Levitan, 2000), 3 min after exposure. This contact time yielded a consistent fertilization curve in preliminary experiments and is appropriate for *L. pictus* (Rosman et al., 2007). Embryos were allowed to develop for 1.5 h, after which they were fixed with 4% formaldehyde in ASW and washed twice with fresh ASW. At least 100 embryos from each replicate were scored for percentage fertilization based on the number of cells showing cleavage. A total of 18 males were used, but one male was excluded from analyses because of extremely low fertilization (<5%). To compare male performance within each trial, relative male fertilization success was calculated as mean % eggs fertilized by male 1/mean % eggs fertilized by male 2 for each pair of males within a single trial (Tvedt et al., 2001).

Lytechinus pictus eggs contain speract, a well-studied peptide that acts as a sperm attractant (Shimomura et al., 1986; Garbers et al., 1982; Guerrero et al., 2010). Elastase (>99% purity; Promega Corporation, Madison, WI, USA), an enzyme that cleaves at the C-terminus of the amino acids valine, glycine and leucine (Narayanan and Anwar, 1969), was utilized to selectively remove the speract (Gly-Phe-Asp-Leu-Asn-Gly-Gly-Gly-Val-Gly; Garbers et al., 1982) attractant around live eggs (Fig. 1A). Elastase was diluted to 10^{-7} mol l^{-1} in ASW for use in trials, and was also denatured by heating 5 ml of the diluted enzyme to boiling and used as a control for the effects of adding the enzyme material to eggs. Eggs used for enzyme assays were spawned directly into beakers containing 5×10^{-2} mol l^{-1} Tris in ASW. Eggs from 2–4 females were pooled together in equal ratios to minimize individual female variability, and 10 ml was put into each of three 40 ml conical tubes. One tube received 0.5 ml of elastase, one tube received 0.5 ml of denatured elastase and the control tube received 0.5 ml of ASW. The eggs were incubated for 1.5 h before being used in a fertilization assay. The change in percentage fertilization between treatments was determined using a random-intercepts mixed effects model (Zuur et al., 2009), with individual males as a random effect and sperm:egg ratio and treatment as fixed effects (package lme4; Bates et al., 2014; R Core Team, 2013). Percentage change in fertilization was calculated as: (% eggs fertilized in control condition−% eggs fertilized in treatment condition)/% eggs fertilized in control condition. Prior to testing, high performance liquid chromatography and mass spectrometry (HPLC-MS) was used to confirm that elastase digests both synthetic and egg-associated speract (Fig. 2). Egg-associated speract was prepared for this test by centrifuging eggs and desalting the resulting egg-conditioned seawater with a Sep-Pak C18 Plus Light column (Waters Corporation, Milford, MA, USA). The column was cleaned with 3 ml

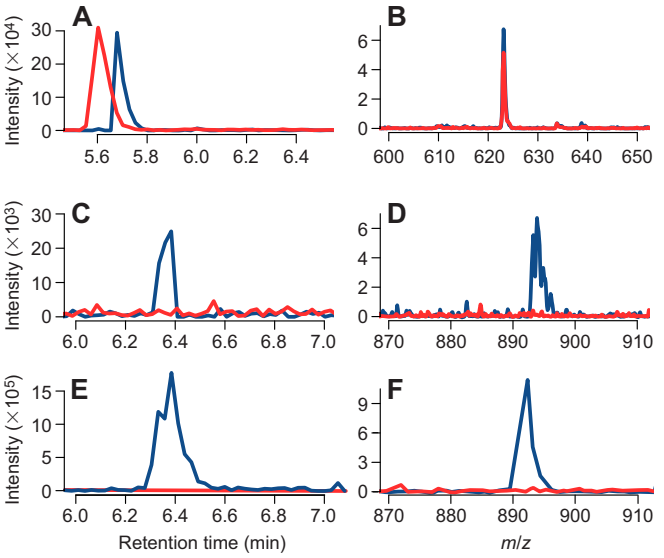

Fig. 2. HPLC-MS data show purified and native speract is digested by the enzyme elastase while the peptide resact, used as an internal standard, remains. Blue denotes data from the control condition (without elastase) and red denotes data from the elastase-incubated solution. Intensity is given in arbitrary units. (A) Extracted ion chromatogram for 622–623 *m*/*z* (mass/charge ratio), corresponding with the primary peak of the internal standard resact, which is retained between the control and elastase-incubated conditions. (B) Mass spectrum of the retention time corresponding with the primary peak of the internal standard resact. The mass fragmentation of resact is identical in the control and elastase conditions. (C) Extracted ion chromatogram for 893–894 *m*/*z*, corresponding with the primary peak of the sperm chemoattractant speract, which is digested in the elastase-incubated (red) condition. (D) Mass spectrum of the retention time corresponding with the primary peak of speract, showing that speract is no longer present in the elastase-incubated (red) condition. (E) Eggs from two *Lytechinus pictus* females were incubated in ASW with elastase (red) or without elastase (blue). Speract appears in the control condition and does not appear in the elastase-incubated solution, indicating that native speract is digested by elastase. (F) Mass spectrum of the retention time corresponding with the primary peak of speract in egg-conditioned seawater, showing that speract is no longer present around eggs incubated in elastase.

of 50% acetonitrile (ACN) in Milli-Q water and equilibrated with 3 ml of Milli-Q water at a flow rate of 1 ml min^{-1}. Egg-conditioned seawater was loaded on to the column at 0.3 ml min^{-1}, washed with 1.2 ml of Milli-Q water, and eluted at 0.3 ml min^{-1} with 1 ml of 25% ACN with 1% acetic acid. The eluted sample was lyophilized and reconstituted in 100 µl of Milli-Q water. The effects of elastase on gamete viability were also examined; sperm exposed to a gradient of speract plus elastase had a distribution in the microfluidic device that was not significantly different from that in the ASW control (Student's *t*-test, all $P>0.1$, Fig. 3A). In addition, to determine whether elastase influenced sperm motility, sperm were exposed to elastase or ASW in the microfluidic device and the linear velocity of the cells was quantified. The results showed that cell velocities were not significantly different between the ASW and elastase treatments (Student's *t*-test, $N=52$ sperm, $P>0.10$; Fig. 3B). The effects of elastase on egg viability and embryo development were determined by incubating eggs in elastase or ASW, adding sperm to a gamete ratio of 300 sperm per egg, and examining the plutei larvae 69 h post-fertilization; no morphological differences were found (Fig. 3C).

Microfluidics and imaging

We designed a microfluidic device that enabled us to expose sperm from different males to the same precisely controlled chemoattractant gradient (Fig. 1C) and compare sperm behavior

Journal of Experimental Biology (2016) 219, 1458-1466 doi:10.1242/jeb.134924

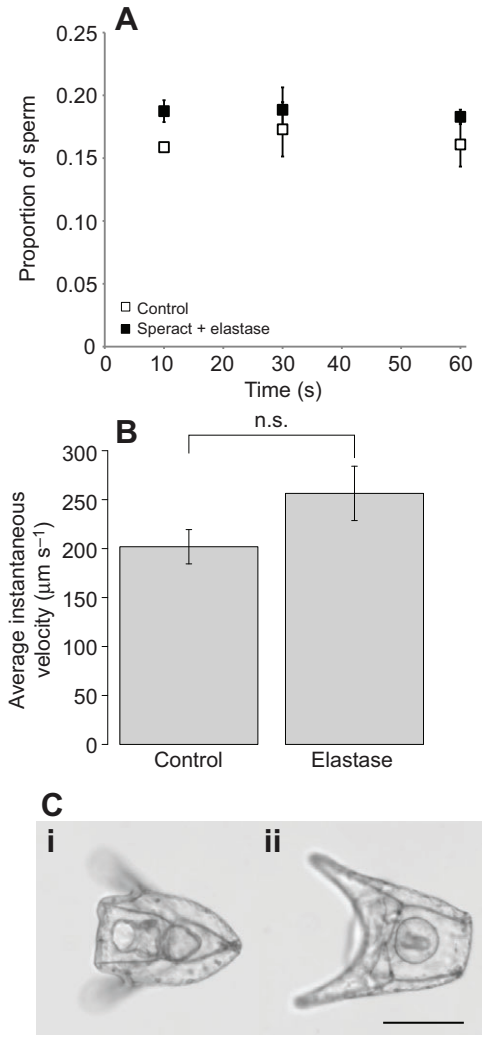

Fig. 3. Elastase negates the effect of speract on sperm distribution, and does not affect sperm motility or embryo development. (A) The distribution of sperm in ASW does not significantly differ from the distribution of sperm in a speract–elastase mixture (Student's *t*-test, all $P>0.1$). (B) Sperm motility does not change in ASW containing elastase, as compared with sperm motility in an ASW control. The mean velocity of sperm in the control and elastase treatments is not significantly different (Student's *t*-test, $N=52$ sperm, 26 per treatment, $P=0.104$). (C) Eggs incubated in ASW with elastase (ii) develop to the pluteus larval stage identically to eggs incubated in ASW without elastase (i). Scale bar, ~100 μm.

between males. As previously described (Ahmed and Stocker, 2008), polydimethylsiloxane (PDMS) channels were designed using CAD software (Autodesk, San Rafael, CA, USA), printed onto transparency film with a high-resolution image setter (Fineline Imaging, Colorado Springs, CO, USA), and patterned onto a 4 in silicon wafer, which was spin-coated with 99 μm-thick negative photoresist (SU8-2100; Microchem, Newton, MA, USA), by exposure to ultraviolet light. The patterned channel structure had three input branch channels that met in a single 'test' channel that was 4 cm long, 99 μm deep and 1020 μm wide. PDMS (Dow Corning, Midland, MI, USA) was molded against the silicon master, cured at 22°C for 24 h, peeled off of the silicon mold and cut to the size of a standard glass slide (25×75 mm). Inlets and outlets were punched into the channel using a 1 mm Harris micro-punch (Ted Pella, Redding, CA, USA) and attached to a glass slide. A covalent bond between the PDMS channel and glass slide was established by pretreating both with oxygen plasma and baking the bonded channel at 60°C for 1 h.

The microfluidic device was placed on an inverted microscope (Nikon TE2000; Nikon Instruments, Melville, NY, USA) equipped with a 10× Nikon Plan Fluor objective. Non-toxic polyethylene tubing (BD Intramedic™, Franklin Lakes, NJ, USA) was inserted into input channels and attached to 1 ml gastight syringes (Hamilton Company, Reno, NV, USA) containing ASW, sperm diluted 1000× (~1×10^7 to ~5×10^7 sperm ml^{-1}) in ASW, or the attractant speract (Phoenix Pharmaceuticals, Burlingame, CA, USA) diluted to 1.39×10^{-9} mol l^{-1} in ASW. Experiments began an average of 5 min after sperm dilution. Bubbles were removed from the syringes and tubing prior to each experiment. A syringe pump (Harvard Apparatus, Holliston, MA, USA) was used to apply a flow rate of 10 μl min^{-1} for 60 s to keep the cells and attractant stratified. Stopping the flow allowed the attractant gradient to develop by diffusion, and video recording began simultaneously. Sperm were imaged mid-depth in the channel using phase-contrast microscopy by recording sequences of 1980 frames at 33 frames s^{-1} with a 512×512 pixel (field of view: 8.2×8.2 mm) CCD camera (iXon Ultra 897; Andor Technology, Belfast, UK). Image analysis software (Nikon-NIS Elements; Nikon Instruments) and MATLAB (MathWorks, Natick, MA, USA) were used to quantify sperm chemosensory behavior (detailed below). The concentration field of speract $c(x,t)$ was obtained from the solution of the advection–diffusion equation (Ahmed et al., 2010) and verified using epifluorescence images of 10^{-4} mol l^{-1} fluorescein (Fluka), which was used as a proxy for the attractant in the microfluidic channels. To account for the difference in diffusion coefficients between fluorescein ($D=5\times10^{-10}$ m^2 s^{-1}; Qasaimeh et al., 2011) and speract ($D=3\times10^{-10}$ m^2 s^{-1}; Guerrero et al., 2013), time was scaled by the ratio of their diffusion coefficients.

Chemotaxis assays and analysis

Microfluidic chemotaxis assays were performed by injecting sperm diluted 1000× into the middle input port, ASW into a side input port, and 1.39×10^{-9} mol l^{-1} speract into the opposite side input port (Fig. 1C). No-speract controls were run in parallel, with ASW injected into both side input ports. After video collection, custom-written scripts in MATLAB (MathWorks) and R (R Core Team, 2013) were used to analyze the trajectories of the sperm tracks. Analyses included distribution of sperm within the channel, as well as track orientation with respect to the attractant gradient direction (0 deg). In *L. pictus* sea urchins, the relationship of chemokinesis and chemotaxis is unclear (Chang et al., 2013; Shiba et al., 2008). We thus conducted a preliminary analysis of sperm from 10/18 males; the results showed no evidence for speract influencing cell velocities compared with the ASW control (paired *t*-test, $P=0.92$; mean±s.e.m. for the speract treatment: 167.7± 70.7 μm s^{-1}; ASW treatment: 166.5±58.7 μm s^{-1}).

For sperm distribution analysis, the locations of all visible sperm were marked at 10, 30 and 60 s after stopping flow, and cells stuck to the bottom of the channel were excluded from analysis. The proportion of sperm in the attractant (or control) location at each time point was calculated by dividing the number of sperm in the attractant side (1/3) of the channel by the total number of sperm in the channel. To compare paired male performance within the same trial, the proportion of sperm in the attractant stream for male 2 was subtracted from that of male 1 (Gage et al., 2004).

For orientation analysis, the trajectories of 6–28 sperm per treatment per male were digitized and the first and last points of each track were used to determine the vector length, calculated as $r=\sqrt{(\Delta x)^2+(\Delta y)^2}$, and orientation, calculated as

Journal of Experimental Biology (2016) 219, 1458-1466 doi:10.1242/jeb.134924

$\theta_s = \tan^{-1}(\Delta y/\Delta x)$, of the full trajectory. The orientation of all sperm tracks in each treatment, reflected about the *x*-axis to yield a range of 0–180 deg, was pooled and used to test the difference between sperm orientation under control and attractant conditions. The mean orientation (θ) and mean resultant vector length (ρ) of all sperm from each male were calculated using the CircStats (Lund and Agostinelli, 2001; Jammalamadaka and Gupta, 2001) package in R (R Core Team, 2013). The mean orientation of sperm in the attractant treatment (θ_a) was used to compare sperm orientation between males. To compare paired male performance within the same trial, relative orientation was calculated as $\theta_{a,male1} - \theta_{a,male2}$. We also computed a preference index (PI) for each male, in which PI=[number of sperm oriented towards the attractant (θ_a<90 deg) −number of sperm oriented away from the attractant (θ_a>90 deg)]/(total number of sperm) (Vinauger et al., 2014). The index takes a value of PI=1 when all sperm are oriented towards the attractant and PI=−1 when all sperm are oriented away from the attractant.

RESULTS

Contribution of the sperm chemoattractant speract and inter-male variation to fertilization success

To identify the degree to which sperm chemotactic ability may influence fertilization, we manipulated the attractant plumes around live eggs by exposing eggs to an enzyme (elastase) that selectively digests the chemoattractant (Fig. 2). As a control, we determined that elastase had no effect on gamete viability and embryo development (Fig. 3). Using a range of sperm:egg ratios that spans from sperm-limited (100:1 sperm:egg) to -saturated (1000:1 sperm:egg) conditions, we measured the difference in fertilization success between treatments for each male and for all males in the experiment. For one representative male (Fig. 4A), the percentage of eggs fertilized in ASW (first control) was 13.5% higher than in the elastase treatment [confidence interval (CI) −19.2, −7.9; ANCOVA, Tukey *post hoc* test, P<0.001] and the percentage of eggs fertilized after incubation in denatured elastase (second control) was not significantly different from that in the ASW treatment (ANCOVA, Tukey test, P=0.47). For another representative male (Fig. 4B), the percentage fertilization for eggs in ASW was 4.6% higher (CI −9.0, −0.28) than for eggs incubated in elastase (ANCOVA, Tukey test, P<0.05), and the percentage fertilization of the two controls (ASW, denatured elastase) did not significantly differ (ANCOVA, Tukey test, P=0.47). Individual male differences have a significant effect on fertilization (ANOVA for male effect, P<0.001). Therefore, we analyzed the data from all 8 males with a random-intercepts mixed-effects model (Zuur et al., 2009) with male as the random effect, and sperm:egg ratio and treatment as fixed effects.

We found that, for all individual males combined (Fig. 4C), elastase lowered fertilization by 5.1% (CI −7.76, −2.51; N=532, P<0.001), a 22.4% change in fertilization from the ASW control. Using the same model, we found that denatured elastase did not affect fertilization (CI −2.43, 2.82; N=532 trials, P=0.88). We tested adding an interaction between sperm:egg ratio and treatment to the model and found no significant interaction (ANOVA of models with and without interaction, P=0.26). However, the treatment effect at the sperm:egg ratio of 300 sperm per egg is larger than the model average, as elastase lowers fertilization by 8.5%, which is a 37.5% change in fertilization from the seawater control (Student's *t*-test, P=0.05, Bonferroni-corrected *P*-values, N=8 males with 8 fertilization replicates per treatment per male (for 3 males, 3 replicates per treatment per male). At the sperm-limited gamete ratio of 100 sperm per egg and at the sperm-saturated gamete ratio of 1000 sperm per egg, there is no statistically significant difference between fertilization in control and elastase conditions (P=1.0 and 0.63, respectively). Our data show that removing chemoattractant from live eggs decreases fertilization success, especially at intermediate sperm/egg concentrations.

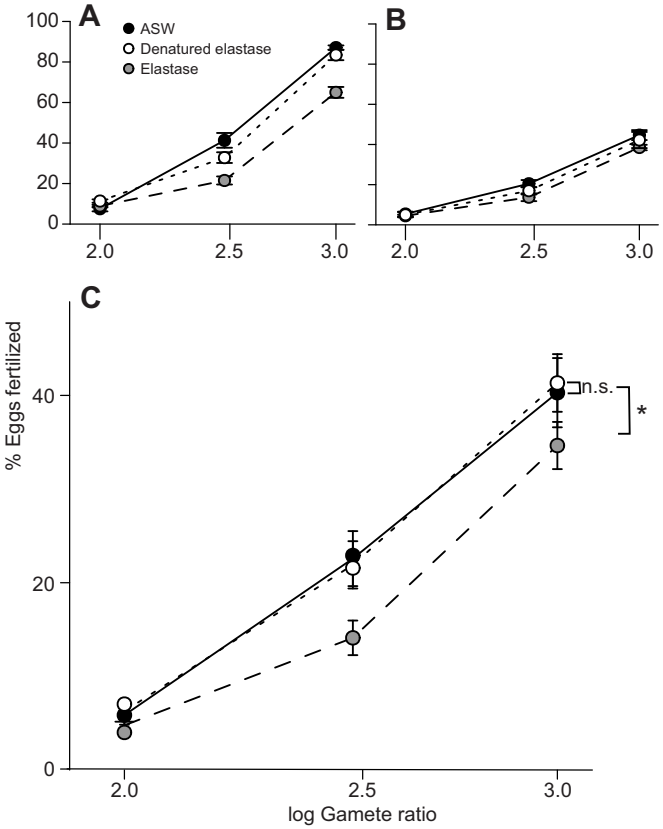

Fig. 4. Effect of elastase on fertilization rates. (A) Fertilization curve for one male fertilizing eggs incubated with ASW (control), elastase or denatured elastase (second control). (B) Fertilization curve for another representative male fertilizing eggs in ASW, elastase or denatured elastase. (C) Combined mean fertilization curves of all males fertilizing eggs incubated with ASW, elastase or denatured elastase. Elastase yielded a change in fertilization of 22.35% (N=532, P<0.001) and denatured elastase did not affect fertilization (P=0.88). At a log sperm:egg ratio of 2.5, elastase yields a percentage change of fertilization of 37.5% (N=113, *P=0.05). At log sperm:egg ratios of 2.0 and 3.0, there is no statistically significant difference between fertilization rates in control and elastase conditions (P=1.0 and 0.63). Error bars indicate ±s.e.m.

Relationship between individual fertility and sperm chemotactic behavior

In order to determine the effect of sperm chemotactic behavior on individual male fertilization success, we compared the fertilization success of males paired with the same group of eggs to the chemotactic ability of sperm from the same males. Sperm chemotactic ability was measured for a subpopulation of sperm from individual males using a microfluidic chemotaxis assay. A chemoattractant gradient was formed by stopping a controlled, laminar flow within a microfluidic device and allowing diffusion to occur (see Materials and methods for details). To identify how the entire sperm population from a male responds to the attractant gradient, we examined the spatial distribution of sperm within the channel at 10, 30 and 60 s after the gradient was initiated. The distribution of sperm in the channel differed significantly between the control and attractant conditions, where sperm aggregate in the region of the channel with a high concentration of attractant (Fig. 5).

Journal of Experimental Biology (2016) 219, 1458-1466 doi:10.1242/jeb.134924

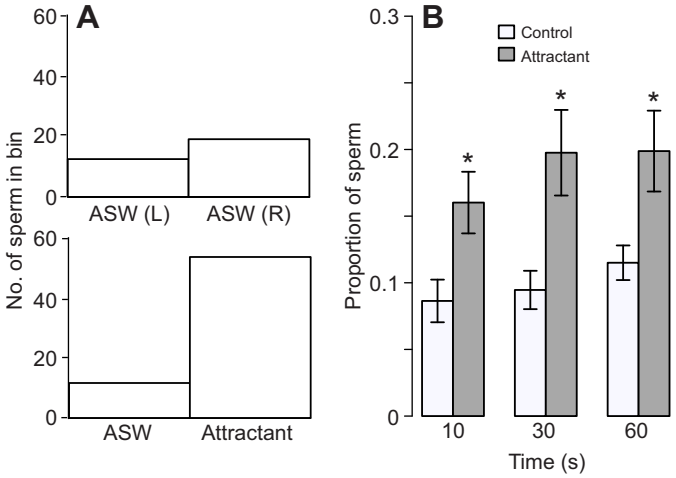

Fig. 5. Changes in sperm distribution between control and attractant conditions. (A) In a representative experiment, sperm significantly redistribute into the attractant side of the channel (bottom), as compared with the distribution in the control condition when the attractant is replaced by ASW (top). (B) In all trials, at 10, 30 and 60 s after flow is stopped in the microfluidic channel, the proportion of sperm in the attractant side of the channel is higher than that in the control (when no attractant is present; Student's *t*-tests, N=17 males, *P<0.05). Error bars indicate ±s.e.m.

For individual males, the number of sperm cells in the attractant side of the channel was higher than in control experiments where the attractant was replaced with ASW (e.g. Fig. 5A). For all males combined, the proportion of sperm in the attractant side of the channel was significantly higher than that in the control channel, at all time points (e.g. at 10 s, proportion in attractant=0.16, in control=0.09; *t*-tests, N=17 males, all P<0.05; Fig. 5B). As a result of differences in baseline fertilization ability for trials completed during different times in the gravid season, we investigated the impact of sperm behavior on fertilization differences within trials of paired males. Differences in fertilization between males were significantly correlated with sperm distribution in the attractant stream (linear regression, slope=1.28, N=8 pairs, 16 males, R^2=0.62, P<0.05; Fig. 6A).

To quantify single-sperm behavior, we considered the orientation of sperm tracks towards the attractant source. We verified that the mean whole-track sperm orientation θ (0–180 deg), calculated by CircStats (Lund and Agostinelli, 2002) in R (R Core Team, 2013), became closer to 0 deg (the direction of the attractant source) in response to the application of a chemoattractant gradient (Fig. 7A,B; Wilcoxon test, P<0.001, N=345 sperm tracks in attractant and 316 sperm in control from 17 males). Sperm exposed to the attractant oriented and exhibited a higher preference index than sperm exposed to the ASW control (PI attractant=0.34±0.06, PI control=0.04±0.07, paired *t*-test, N=17 males, P<0.01; Fig. 7D). Individual males differed in their mean sperm orientation θ_a (Fig. 7C), but these differences were not statistically significant (ANOVA of θ_a with male as the factor, P=0.17). We then examined the relationship of the relative fertilization success of males paired by trial with the relative mean orientation of sperm towards the attractant source (0 deg). Differences in fertilization ability had an inverse relationship with sperm orientation towards the attractant θ_a (Fig. 6B), but this effect was not statistically significant (linear regression, slope=−0.02, N=8 pairs, 16 males, R^2=0.30, P=0.16). Our data show that sperm movement towards the chemoattractant source partially explains differences in male fertilization success.

DISCUSSION

In this study, we investigated the effect of sperm chemotaxis on fertilization success using two distinct approaches. In the first approach, we compared fertilization ability with and without an enzyme that digests the sperm chemoattractant speract. In the second approach, we coupled fertilization assays with a novel chemotaxis assay in a microfluidic device (Fig. 1) to compare the fertilization success and chemotactic performance of paired males fertilizing the same group of eggs. We found that removing the sperm chemoattractant decreased fertilization success (Fig. 4) and that sperm movement towards the chemoattractant correlated with relative male fertilization success (Fig. 6).

Removing speract from live eggs led to an overall percentage decrease in fertilization of 22.4%. This difference is significant, and may compound with other selection mechanisms in sperm competition, such as sperm longevity (Levitan, 2000) and gamete recognition proteins (Swanson and Vacquier, 2002; Palumbi, 1999; Evans and Sherman, 2013; Levitan, 2012). Gamete recognition proteins are a particularly important prezygotic mediator of fertilization success. The gamete recognition proteins bindin (on sperm; Vacquier and Moy, 1977) and EBR1 (on eggs; Foltz and Lennarz, 1990) mediate both interspecies and intraspecies gamete compatibility (Palumbi, 1999; Zigler et al., 2005). This known influence on fertilization, coupled with extensive evidence that gamete recognition factors evolve more quickly than other proteins (Swanson and Vacquier, 2002), implies that gamete recognition proteins are a crucial component of fertilization success, operating downstream of water-borne sperm attractants. Our current study

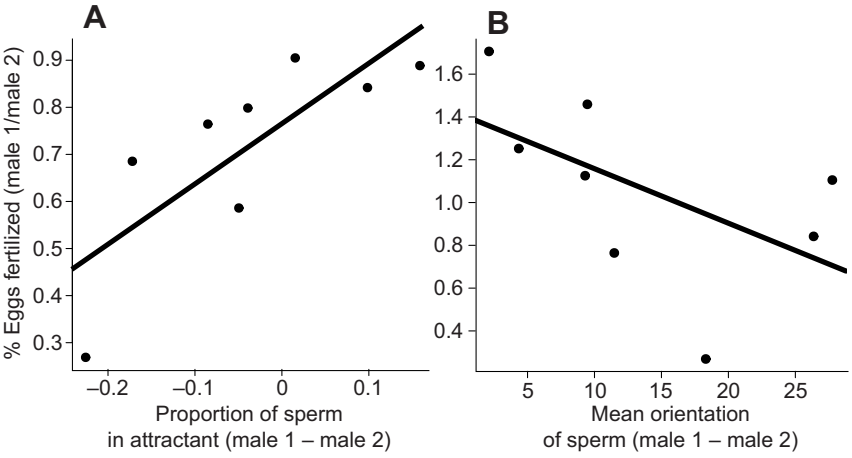

Fig. 6. Relative fertilization success related to sperm chemotactic parameters. (A) Relative fertilization success of individual males paired by trial, varying by the relative proportion of sperm in the attractant stream at 10 s post-attractant exposure. Differences in fertilization rates are explained by sperm distribution in the attractant stream (linear regression, slope=1.28, N=8 pairs, 16 males, R^2=0.62, P<0.05). (B) Relative fertilization success of individual males paired by trial, varying by the relative mean orientation of sperm towards the attractant source. We expect an inverse relationship, as 0 deg is the direction of the attractant source. Differences in fertilization rates seem to be explained by sperm orientation towards the attractant, but the relationship is not statistically significant (linear regression, slope=−0.02, N=8 pairs, 16 males, R^2=0.30, P=0.16).

Journal of Experimental Biology (2016) 219, 1458-1466 doi:10.1242/jeb.134924

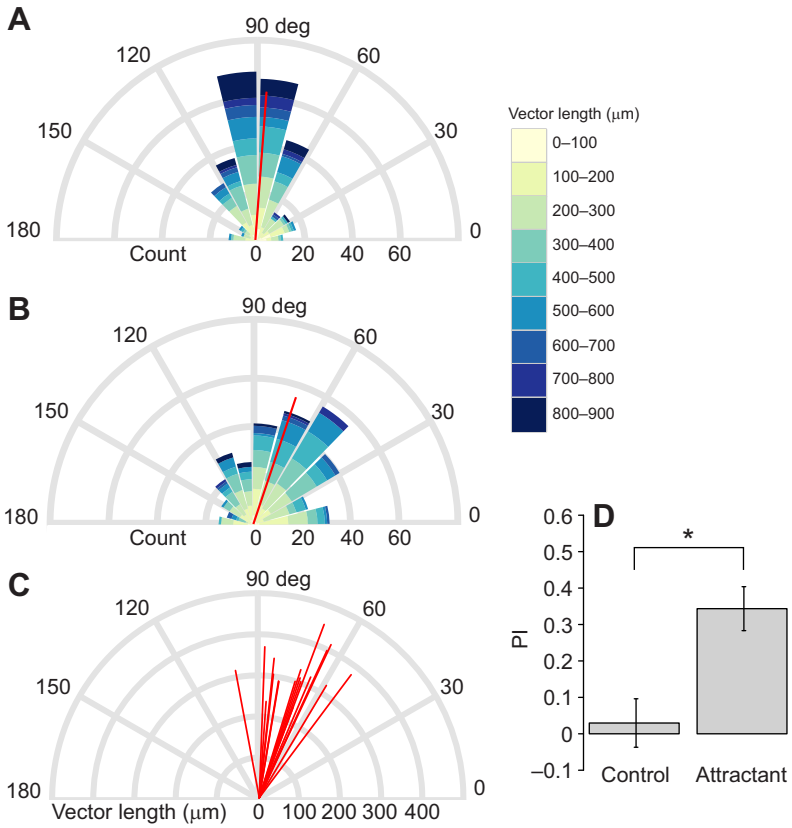

Fig. 7. Sperm orientation in the microfluidic channel. Angle θ=0 deg is the direction of the attractant source. (A) In the no-speract control, the mean sperm direction θ is 88.3 deg and the mean resultant vector length ρ is 0.82 (scaled to maximum count; *N*=316 sperm from 17 males). (B) The mean sperm orientation to attractant θ_a is 72.7 deg and the mean resultant vector length ρ is 0.74 (scaled to maximum count; *N*=345 sperm from 17 males). (C) Mean resultant vectors (ρ) of mean sperm orientation of each male to the attractant. (D) Preference index (PI) of sperm in the control and attractant conditions, where positive preference index indicates a higher proportion of sperm moving towards the attractant side of the channel. Sperm have a higher PI towards attractant than to an ASW control (PI attractant=0.34, PI control=0.04, paired *t*-test, *N*=17 males, **P*<0.01).

provides the impetus for determining the relative contributions of gamete recognition proteins and sperm chemotaxis to individual male fitness.

Digestion of the chemoattractant around eggs had the greatest effect when sperm:egg ratios were at the intermediate (300:1) gamete ratio, where we found a 37.5% change in fertilization; when sperm were limiting (100:1) or saturating (1000:1), loss of chemoattractant had less of an effect. These results are similar to previous work where Riffell et al. (2004) found that chemoattraction did not affect fertilization under sperm-limiting and sperm-saturating conditions. Our data show that the chemoattractant speract is an important factor mediating *L. pictus* gamete interactions and fertilization success.

As a result, we considered differences in sperm chemotactic ability and their effect on individual male fitness. Microfluidics allowed us to reproducibly control the spatial and temporal gradient of speract chemoattractant that sperm were experiencing and simultaneously visualize sperm population dynamics and individual sperm behavior (Ahmed et al., 2010). Microfluidic chemotaxis assays showed that more sperm oriented to and migrated towards the chemoattractant than to seawater. The population-level indicator of cell accumulation and the single-cell indicator of swimming orientation demonstrate that sperm chemotaxis can be robustly measured in our microfluidic device.

The proportion of sperm migrating to the attractant stream correlated significantly with the relative fertilization success of paired males, indicating that the ability of sperm to move towards their chemoattractant reflects their ability to fertilize eggs. This result reveals a direct connection between sperm chemotactic behavior and male reproductive success, and builds upon previous studies which found that chemoattraction increases gamete encounters (Riffell et al., 2004) and connected sperm preference for particular eggs to gamete compatibility and conspecific recognition (Evans et al., 2012; Oliver and Evans, 2014). The present study is the first to demonstrate that differences in individual male fertilization success are correlated with differences in sperm chemotaxis.

Interestingly, we did not find a significant correlation between mean orientation of sperm towards the attractant and relative fertilization success of paired males. Sperm orientation may be a weaker indicator of chemotactic ability than sperm distribution because sperm traveling at any angle between 0 and 90 deg will reach the attractant source. We also may not have captured the full extent of sperm recruitment towards the attractant, as the approximately 3 s delay between stopping flow and the cessation of fluid motion may have been enough time for sperm to adapt to the attractant before being captured in our tracking algorithm. Nonetheless, the relationship between sperm distribution and male fertilization success and the change in orientation by sperm in the presence of the attractant indicate that sperm chemoattraction is an important contributor to fertilization success.

Sperm competition and chemoattraction

Once gametes from broadcast-spawning invertebrates such as sea urchins are released into the ocean, their variable fertilization success leads directly to differences in reproductive success between males (Fitzpatrick and Lüpold, 2014; Evans et al., 2012). The large scale of the ocean environment, which dilutes gametes, and its frequently turbulent nature, which can affect motility, creates strong selective pressure on gamete traits. Sperm traits are thus vital in promoting gamete encounters in the water column, and there is evidence that traits such as sperm motility and morphology often correlate with male reproductive success (Fitzpatrick and Lüpold, 2014; Snook, 2005; Simmons and Fitzpatrick, 2012). Evidence from multiple marine

organisms, including broadcast-spawning mussels and internally and externally fertilizing fish, suggests that sperm chemoattraction is under selective pressure (Evans and Sherman, 2013). Previous studies found a correlation between sperm chemoattraction to specific eggs and the ability of the eggs to be fertilized, both in broadcast-spawning marine invertebrates (Krug et al., 2009; Evans et al., 2012) and humans (Ralt et al., 1991), providing evidence for chemoattraction as a signal of gamete viability and compatibility. In this study, the significant effect of chemoattraction on fertilization success reinforces our understanding of chemotaxis as a trait with the potential for selection. The ubiquity of sperm chemoattraction in divergent taxa and the species specificity of chemoattractant signaling molecules (Miller, 1997; Riffell et al., 2004; Yoshida et al., 2013) suggest a role for chemoattraction in reproductive isolation and species evolution.

Summary

Using a chemoattractant-digesting peptidase and a microfluidic device coupled with fertilization assays, we show that sperm chemotactic ability affects individual male fertilization success in the sea urchin *L. pictus*. Removing chemoattractant from a group of eggs leads to a decrease in the percentage of eggs that are fertilized. Sperm change their distribution and orientation in response to the application of a chemoattractant gradient generated within a microfluidic device. Individual male sperm distribution in the channel at 10 s post-exposure to attractant correlates with fertilization success, results which are particularly important for broadcast-spawning marine invertebrates, where fertilization is rapid. Sperm chemotaxis is common throughout sexually reproducing organisms (Eisenbach, 1999; Yoshida, 2014), including humans, and our results indicate that microfluidic chemotaxis assays could be used to test male fitness. Our study demonstrates for the first time that sperm chemotaxis influences individual fertilization success, implying that sperm chemoattraction is a trait under selection and providing the impetus for investigating the relative contributions of sperm chemotaxis and other gamete traits to fertilization.

Acknowledgements

We thank S. Salad for assistance with experiments and video analysis, M. Sadilek and L. Vandepas for technical assistance, J. Cerchiara, M. Clifford and M. Roberts for comments on the manuscript, and L. Love-Anderegg, I. Breckheimer and the UW Biostatistics Consulting Center for statistics advice.

Competing interests

The authors declare no competing or financial interests.

Author contributions

Y.H.H., R.K.Z. and J.A.R. designed the study; J.S.G. and R.S. developed microfluidic and imaging tools for the study; Y.H.H. carried out experiments and analyzed the data. Y.H.H., J.A.R., J.S.G., R.S. and R.K.Z. wrote the manuscript. All authors gave final approval for publication.

Funding

This work was funded by the National Science Foundation Division of Integrative Organismal Systems under grants IOS-1121692 (J.A.R., R.S., R.K.Z.) and IOS-1354159 (J.A.R.). This work was also supported by the University of Washington Endowed Chair for Excellence in Biology (J.A.R.), the National Science Foundation Graduate Research Fellowship Program under grant no. DGE-1256082, an Achievement Rewards for College Scientists (ARCS) Foundation Fellowship, and the University of Washington Department of Biology Edmondson Award (Y.H.H.).

Data availability

The datasets supporting this article are available on request from the corresponding author.

References

Ahmed, T. and Stocker, R. (2008). Experimental verification of the behavioral foundation of bacterial transport parameters using microfluidics. *Biophys. J.* **95**, 4481-4493.

Ahmed, T., Shimizu, T. S. and Stocker, R. (2010). Microfluidics for bacterial chemotaxis. *Integr. Biol.* **2**, 604-629.

Bates, D., Maechler, M., Bolker, B. and Walker, S. (2015). Fitting linear mixed-effects models using lme4. *J. Stat. Soft.* **67**, 1-48.

Birkhead, T. and Moller, A. ed. (1998). External fertilizers. In *Sperm Competition and Sexual Selection*, pp. 177-191. San Diego, California: Academic Press.

Brokaw, C. J. (1957). Chemotaxis of bracken spermatozoids. *J. Exp. Biol.* **35**, 192-196.

Chang, H., Kim, B. J., Kim, Y. S., Suarez, S. S. and Wu, M. (2013). Different migration patterns of sea urchin and mouse sperm revealed by a microfluidic chemotaxis device. *PLoS ONE* **8**, e60587.

Darszon, A., Guerrero, A., Galindo, B. E., Nishigaki, T. and Wood, C. D. (2008). Sperm-activating peptides in the regulation of ion fluxes, signal transduction and motility. *Int. J. Dev. Biol.* **52**, 595-606.

Eisenbach, M. (1999). Sperm chemotaxis. *Rev. Reprod.* **4**, 56-66.

Engqvist, L. (2013). A general description of additive and nonadditive elements of sperm competitiveness and their relation to male fertilization success. *Evolution Int. J. Org. Evolution* **67**, 1396-1405.

Evans, J. P. and Sherman, C. D. H. (2013). Sexual selection and the evolution of egg-sperm interactions in broadcast-spawning invertebrates. *Biol. Bull.* **224**, 166-183.

Evans, J. P., Garcia-Gonzalez, F., Almbro, M., Robinson, O. and Fitzpatrick, J. L. (2012). Assessing the potential for egg chemoattractants to mediate sexual selection in a broadcast spawning marine invertebrate. *Proc. R. Soc. B Biol. Sci.* **279**, 2855-2861.

Fitzpatrick, J. L. and Lüpold, S. (2014). Sexual selection and the evolution of sperm quality. *Mol. Hum. Reprod.* **20**, 1180-1189.

Fitzpatrick, J. L., Simmons, L. W. and Evans, J. P. (2012). Complex patterns of multivariate selection on the ejaculate of a broadcast spawning marine invertebrate. *Evolution* **66**, 2451-2460.

Foltz, K. R. and Lennarz, W. J. (1990). Purification and characterization of an extracellular fragment of the sea urchin egg receptor for sperm. *J. Cell Biol.* **111**, 2951-2959.

Gage, M. J. G., Macfarlane, C. P., Yeates, S., Ward, R. G., Searle, J. B. and Parker, G. A. (2004). Spermatozoal traits and sperm competition in Atlantic salmon. *Curr. Biol.* **14**, 44-47.

Garbers, D. L., Watkins, H. D., Hansbrough, J. R., Smith, A. and Misono, K. S. (1982). The amino acid sequence and chemical synthesis of speract and of speract analogues. *J. Biol. Chem.* **257**, 2734-2737.

Guerrero, A., Nishigaki, T., Carneiro, J., Yoshiro Tatsu, J., Wood, C. D. and Darszon, A. (2010). Tuning sperm chemotaxis by calcium burst timing. *Dev. Biol.* **344**, 52-65.

Guerrero, A., Espinal, J., Wood, C. D., Rendon, J. M., Carneiro, J., Martinez-Mekler, G. and Darszon, A. (2013). Niflumic acid disrupts marine spermatozoan chemotaxis without impairing the spatiotemporal detection of chemoattractant gradients. *J. Cell Sci.* **126**, 1477-1487.

Hansbrough, J. R. and Garbers, D. L. (1981). Speract: purification and characterization of a peptide associated with eggs that activates spermatozoa. *J. Biol. Chem.* **256**, 1447-1452.

Harvey, E. B. (1956). *The American Arbacia and Other Sea Urchins*. Princeton, NJ: Princeton University Press.

Jammalamadaka, S. R. and Gupta, A. S. (2001). *Topics in Circular Statistics*. River Edge, NJ: World Scientific Publishing Co.

Johnson, D. W., Monro, K. and Marshall, D. J. (2013). The maintenance of sperm variability: context-dependent selection on sperm morphology in a broadcast spawning invertebrate. *Evolution* **67**, 1383-1395.

Kaupp, U. B., Hildebrand, E. and Weyand, I. (2006). Sperm chemotaxis in marine invertebrates—molecules and mechanisms. *J. Cell. Physiol.* **208**, 487-494.

Kopf, G. S., Tubb, D. J. and Garbers, D. L. (1979). Activation of sperm respiration by a low molecular weight egg factor and 8-bromoguanosine 3′5′-monophosphate. *J. Biol. Chem.* **254**, 8554-8560.

Krug, P. J., Riffell, J. A. and Zimmer, R. K. (2009). Endogenous signaling pathways and chemical communication between sperm and egg. *J. Exp. Biol.* **212**, 1092-1100.

Lessios, H. A., Lockhart, S., Collin, R., Sotil, G., Sanchez-Jerez, P., Zigler, K. S., Perez, A. F., Garrido, M. J., Geyer, L. B., Bernardi, G. et al. (2012). Phylogeography and bindin evolution in *Arbacia*, a sea urchin genus with an unusual distribution. *Mol. Ecol.* **21**, 130-144.

Levitan, D. R. (2000). Sperm velocity and longevity trade off each other and influence fertilization in the sea urchin *Lytechinus variegatus*. *Proc. R. Soc. B Biol. Sci.* **267**, 531-534.

Levitan, D. R. (2012). Contemporary evolution of sea urchin gamete-recognition proteins: experimental evidence of density-dependent gamete performance predicts shifts in allele frequencies over time. *Evolution* **66**, 1722-1736.

Lillie, F. R. (1912). The production of sperm iso-agglutinins by ova. *Science* **36**, 527-530.

Lillie, F. R. (1915). Studies of fertilization. VII. analysis of variations in the fertilizing power of sperm suspensions of *Arbacia*. *Biol. Bull.* **28**, 229-251.

Lund, U. and Agostinelli, C. (2007). CircStats: Circular Statistics. R package version 0.2-3, http://CRAN.R-project.org/package=CircStats.

Metz, E. C., Gómez-Gutiérrez, G. and Vacquier, V. D. (1998). Mitochondrial DNA and bindin gene sequence evolution among allopatric species of the sea urchin genus *Arbacia*. *Mol. Biol. Evol.* **15**, 185-195.
Miller, R. L. (1997). Specificity of sperm chemotaxis among Great Barrier Reef shallow-water holothurians and ophiuroids. *J. Exp. Zool.* **279**, 189-200.
Narayanan, A. S. and Anwar, R. A. (1969). The specificity of purified porcine pancreatic elastase. *Biochem. J.* **114**, 11-17.
Oliver, M. and Evans, J. P. (2014). Chemically moderated gamete preferences predict offspring fitness in a broadcast spawning invertebrate. *Proc. R. Soc. B Biol. Sci.* **281**, 20140148.
Palumbi, S. R. (1999). All males are not created equal: fertility differences depend on gamete recognition polymorphisms in sea urchins. *Proc. Natl. Acad. Sci. USA* **96**, 12632-12637.
Qasaimeh, M. A., Gervais, T. and Juncker, D. (2011). Microfluidic quadrupole and floating concentration gradient. *Nat. Commun.* **2**, 464.
R Core Team (2013). R: A Language and Environment for Statistical Computing. Vienna: R Foundation for Statistical Computing. Available at: http://www.r-project.org/.
Ralt, D., Goldenberg, M., Fetterolf, P., Thompson, D., Dor, J., Mashiach, S., Garbers, D. L. and Eisenbach, M. (1991). Sperm attraction to a follicular factor(s) correlates with human egg fertilizability. *Proc. Natl. Acad. Sci. USA* **88**, 2840-2844.
Riffell, J. A., Krug, P. J. and Zimmer, R. K. (2004). The ecological and evolutionary consequences of sperm chemoattraction. *Proc. Natl. Acad. Sci. USA* **101**, 4501-4506.
Rosman, J. H., Koseff, J. R., Monismith, S. G., Grover, J. (2007). A field investigation into the effects of a kelp forest (*Macrocystis pyrifera*) on coastal hydrodynamics and transport. *J. Geophys. Res.* **112**, 1-16.
Schmell, E., Earles, B. J., Breaux, C. and Lennarz, W. J. (1977). Identification of a sperm receptor on the surface of the eggs of the sea urchin *Arbacia punctulata*. *J. Cell Biol.* **72**, 35-46.
Shiba, K., Baba, S. A., Inoue, T. and Yoshida, M. (2008). Ca^{2+} bursts occur around a local minimal concentration of attractant and trigger sperm chemotactic response. *Proc. Natl. Acad. Sci. USA* **105**, 19312-19317.
Shimomura, H., Suzuki, N. and Garbers, D. L. (1986). Derivatives of speract are associated with the eggs of *Lytechinus pictus* sea urchins. *Peptides* **7**, 491-495.
Simmons, L. W. and Fitzpatrick, J. L. (2012). Sperm wars and the evolution of male fertility. *Reproduction* **144**, 519-534.
Simpson, J. L., Humphries, S., Evans, J. P., Simmons, L. W. and Fitzpatrick, J. L. (2014). Relationships between sperm length and speed differ among three internally and three externally fertilizing species. *Evolution* **68**, 92-104.
Snook, R. R. (2005). Sperm in competition: not playing by the numbers. *Trends Ecol. Evol.* **20**, 46-53.
Spehr, M., Gisselmann, G., Poplawski, A., Riffell, J. A., Wetzel, C. H., Zimmer, R. K. and Hatt, H. (2003). Identification of a testicular odorant receptor mediating human sperm chemotaxis. *Science* **299**, 2054-2058.
Strathmann, M. F. (1987). *Reproduction and Development of Marine Invertebrates of the Northern Pacific Coast*. Seattle, WA: University of Washington Press.
Suzuki, N., Shimomura, H., Radany, E. W., Ramarao, C. S., Ward, G. E., Bentley, J. K. and Garbers, D. L. (1984). A peptide associated with eggs causes a mobility shift in a major plasma membrane protein of spermatozoa. *J. Biol. Chem.* **259**, 14874-14879.
Swanson, W. J. and Vacquier, V. D. (2002). The rapid evolution of reproductive proteins. *Nat. Rev. Genet.* **3**, 137-144.
Tvedt, H. B., Benfey, T. J., Martin-Robichaud, D. J. and Power, J. (2001). The relationship between sperm density, spermatocrit, sperm motility and fertilization success in Atlantic halibut, *Hippoglossus hippoglossus*. *Aquaculture* **194**, 191-200.
Vacquier, V. D. and Moy, G. W. (1977). Isolation of bindin: the protein responsible for adhesion of sperm to sea urchin eggs. *Proc. Natl. Acad. Sci. USA* **74**, 2456-2460.
van der Horst, G. and Maree, L. (2014). Sperm form and function in the absence of sperm competition. *Mol. Reprod. Dev.* **81**, 204-216.
Vinauger, C., Lutz, E. K. and Riffell, J. A. (2014). Olfactory learning and memory in the disease vector mosquito, *Aedes aegypti*. *J. Exp. Biol.* **217**, 2321-2330.
Ward, G. E., Brokaw, C. J., Garbers, D. L. and Vacquier, V. D. (1985). Chemotaxis of *Arbacia punctulata* spermatozoa to resact, a peptide from the egg jelly layer. *J. Cell Biol.* **101**, 2324-2329.
Watkins, H. D., Kopf, G. S. and Garbers, D. L. (1978). Activation of sperm adenylate cyclase by factors associated with eggs. *Biol. Reprod.* **19**, 890-894.
Yoshida, M. (2014). Sperm chemotaxis: the first authentication events between conspecific gametes before fertilization. In *Sexual Reproduction in Animals and Plants* (ed. H. Sawada, N. Inoue and M. Iwano), pp. 3-11. Tokyo: Springer.
Yoshida, M. and Yoshida, K. (2011). Sperm chemotaxis and regulation of flagellar movement by Ca^{2+}. *Mol. Hum. Reprod.* **17**, 457-465.
Yoshida, M., Kawano, N. and Yoshida, K. (2008). Control of sperm motility and fertility: diverse factors and common mechanisms. *Cell. Mol. Life Sci.* **65**, 3446-3457.
Yoshida, M., Hiradate, Y., Sensui, N., Cosson, J. and Morisawa, M. (2013). Species-specificity of sperm motility activation and chemotaxis: a study on ascidian species. *Biol. Bull.* **224**, 156-165.
Zigler, K. S., Mccartney, M. A., Levitan, D. R. and Lessios, H. A. (2005). Sea urchin bindin divergence predicts gamete compatibility. *Evolution* **59**, 2399-2404.
Zuur, A. F., Ieno, E. N., Walker, N., Saveliev, A. A. and Smith, G. M. (2009). *Mixed Effects Models and Extensions in Ecology with R*. New York, NY: Springer New York.